NASA Technical Memorandum 78734

Measurement Techniques and Applications of Charge Transfer to Aerospace Research

Alphonsa Smith

SEPTEMBER 1978

NASA

PROPERTY OF NORTHROP UNIVERSITY

NASA Technical Memorandum 78734

Measurement Techniques and Applications of Charge Transfer to Aerospace Research

Alphonsa Smith
Langley Research Center
Hampton, Virginia

NASA
National Aeronautics
and Space Administration

Scientific and Technical
Information Office

1978

SUMMARY

A technique of developing high-velocity low-intensity neutral gas beams for use in aerospace research problems is described. This technique involves ionization of gaseous species with a mass spectrometer and focusing the resulting primary ion beam into a collision chamber containing a static gas at a known pressure and temperature. Equations are given to show how charge-transfer cross sections are obtained from a total-current measurement technique. Important parameters are defined for the charge-transfer process. An error analysis for the experimental measurement parameters indicates that the fractional measurement error for this technique is in the range of 6 to 17 percent.

INTRODUCTION

Many satellite and reentry probe experiments have encountered serious measurement problems with atomic and molecular gas-surface interactions. A proper technique for studying and solving such problems would be to examine the reactions of energetic atomic and molecular beams impinging on surfaces. In order to do this, techniques must be developed for the generation of neutral atomic and molecular beams with velocities equivalent to those of spaceborne satellites. Charge transfer is one method that can be used to produce neutral molecular beams with velocities suitable for aerospace gas-surface interaction studies. A recent study (ref. 1) has dealt with charge-transfer processes in the symmetric nitrogen system. The objective of that study was to measure energy dependence of charge-transfer cross sections in the range of 9 to 441 eV and to investigate the effects of internal state excitation of the primary ion beam on the charge-transfer process. (This primary ion beam energy could provide neutral particles with velocities in the range of interest for aerospace studies.) In addition to providing essential data on neutral molecular beams, charge-transfer cross sections are needed in calculations dealing with gas transport properties at high temperatures (refs. 2 and 3). There is a renewed interest in the problem of high-energy particle interaction with common vacuum materials such as Pyrex glass, stainless steel, Teflon, gold, titanium, and tungsten. This interest is largely due to the investigation of the upper atmosphere with rocketborne mass spectrometers and total-pressure measuring devices.

Measurement of atomic oxygen concentration at high altitudes (about 150 km) is of great astrophysical interest. However, such measurements are very difficult because of large surface recombination effects. The usual measurement instruments, particularly the mass spectrometer, drastically affect the concentration of oxygen atoms in the sample they are analyzing. Because of this effect, the interaction of atomic oxygen beams with many materials has become a primary interest in aerospace research applications. An example is the interaction of atomic oxygen with tungsten. The reaction of oxygen and oxygen containing molecules at hot tungsten filaments usually found in mass spectrometers and ionization gages has an important influence on the performance of ultrahigh

vacuum systems. Oxygen is known to react preferentially with carbon at the surface of hot tungsten. The interaction of oxygen with pure tungsten is complex. The specific interaction process has been found to depend on the tungsten temperature and oxygen pressure. Evaporation of the vapor species of WO_3 occurs at temperatures above 1200 K, and WO_2 vapor is detectable above approximately 1500 K (ref. 4).

In the investigation of atom-surface interaction, the use of charge-transfer beams with a known intensity and energy distribution becomes particularly interesting. A study can be made by this method, and the time history of a charge-transfer beam using modulation and phase-sensitive detection techniques can be followed. By varying the incident beam translational energy, intensity, and the surface temperature of the interacting material, thermal accommodation coefficients can be determined for a variety of surfaces and gases. By using an incident modulated atomic beam, the probability that an atom will rebound from a surface as a free atom can be measured. From examination of the reflected molecular signal, information on the probability of reassociation at the surface is obtained. The probability that an atom after striking a surface will return to the gas phase as an atom is not clearly understood, particularly for highly reactive atoms such as oxygen.

Another logical extension of charge-transfer technique is the determination of chemical-reaction-rate data in ion-molecule reactions. In order to study chemical-reaction rates, cross-section data are needed. Rate data for a general reaction are given by the equation

$$A^+ + B \rightarrow C^+ + D \tag{1}$$

Such data are needed in many atmospheric studies. Reaction-rate data are related to charge-transfer cross section by the equation (ref. 5)

$$K = \int_0^\infty \int_0^\infty f(v_I)\ f(v_M)\ \sigma(v_r)\ v_r\ d^3v_I\ d^3v_M \tag{2}$$

where

K reaction-rate constant

$f(v_I)$ velocity-distribution function for primary ions

$f(v_M)$ velocity-distribution function for neutral molecules

$\sigma(v_r)$ cross section as function of relative molecular velocity between primary ions and neutral molecules

Chemical-reaction-rate data provide the basis for study of many of the ionic processes in the upper boundary region of the stratosphere. Ionic processes that occur in this region may have a direct influence on the stratosphere. The research apparatus discussed in this paper was designed for ion-neutral reaction study capabilities. A similar laboratory measurement program in gas-phase reaction kinetics could be responsive to specific data needs for both

chemical models and field measurements related to atmospheric research. Primary emphasis could be placed in the acquisition of reaction-kinetics data, including reaction-rate constants, temperature dependence, and product formation. The reliability of several stratospheric reaction schemes could be investigated, with emphasis placed on the completeness of present models. Possible new reactions could be investigated and their relative importance or unimportance determined. The results of laboratory studies would also be helpful in planning laboratory measurements and in focusing them at the most vital needs.

This paper discusses a technique based on the charge-transfer method of generating high-velocity low-intensity neutral gas beams. Important parameters which characterize charge-transfer interactions in gases are also discussed. The symmetric nitrogen system $N_2^+ + N_2 \rightarrow N_2 + N_2^+$ was selected as the study subject only for reasons of specificity in the discussion of certain aspects of charge-transfer reactions. The techniques discussed and the conclusions drawn are not limited to the nitrogen system.

SYMBOLS

Values are given in SI and U.S. Customary Units. The measurements were made in the U.S. Customary Units.

C	conductance, liters/second
I	current, amperes
I(x=0)	current at entrance to charge-transfer cell, amperes
k	Boltzmann constant, 1.38×10^{-16} erg/kelvin
p	pressure, pascals
r_1	radius of inlet aperture to charge-transfer cell, centimeters
r_2	radius of exit aperture to charge-transfer cell, centimeters
T	temperature, kelvins
t	time, seconds
V	volume, centimeters^3
X	measurement parameter (see table I)
x	length of charge-transfer cell, centimeters
σ	cross section, centimeters^2
ϕ	electrical potential, volts

$\Delta\phi$	potential difference between CTCS and CTC, volts

Subscripts:

BF1	beam flag 1
CT	charge transfer
CTC	charge-transfer cell
CTCS	charge-transfer cell screen
F	fast primary ions
f	final
IAV	ion acceleration voltage
IE	ion energy
o	initial
p	porous metal leak
S	saturation

Abbreviations:

BF1	beam flag 1
BF2	beam flag 2
CTC	charge-transfer cell
CTCE	charge-transfer cell enclosure
CTCS	charge-transfer cell screen
FD1	focus deflection for first electrode
FD2	focus deflection for second electrode
FD3	focus deflection for third electrode
FD4	focus deflection for fourth electrode
L1	lens 1
L2	lens 2
R/D	ring-drawout electrode

T1 tube 1

T2 tube 2

T3 tube 3

EXPERIMENTAL APPARATUS

A detailed discussion of the apparatus and operating procedure has been described in reference 1. A short summary is however presented herein.

The experimental system (fig. 1) can be divided for the purpose of discussion into three component parts: mass spectrometer, ion optics, and charge-transfer cell section. The purpose of the mass spectrometer is to provide a mass selected primary ion beam with a known kinetic energy. The mass spectrometer system contained an electron-bombardment ion source, a gas inlet system, a vacuum pumping station, a pressure monitoring system, and electronic controls.

The purpose of the ion-optics section (figs. 2 and 3) is to direct and guide the transport of the primary ion beam from the mass spectrometer analyzer exit at the ring-drawout (R/D) electrode to the charge-transfer cell (CTC). This technique was done by employing conventional ion-optics with lens element of three basic geometric configurations: cylindrical, disk, and flat-plate type. The electrical potentials on all lens elements were separately controlled by regulated power supplies to obtain a stable ion beam of maximum intensity at the CTC section.

The charge-transfer cell section (fig. 4) consists of five parts: the charge-transfer cell (CTC), the charge-transfer cell screen (CTCS), the charge-transfer cell enclosure (CTCE), beam flag 1 (BF1), and beam flag 2 (BF2). This section is utilized to focus, detect, and measure the primary and product ions made in the charge-transfer process. Detection of the ion beam was done by absolute current measurements using three precision electrometers to measure total currents to CTC, CTCS, and BF2. Beam flag 1 is a movable element positioned at the entrance to the charge-transfer cell and is used to help collimate the ion beam into CTC. A thin-edged circular hole, 0.16-cm diameter in BF1 insures that all beam current passing through BF1 enters CTC. The entrance aperture of CTC is also thin edged and is 0.24 cm in diameter. For this application, it is important that the aperture diameter in BF1 be smaller than the entrance aperture diameter of CTC to insure that none of the incoming ion beam is collected on the entrance aperture of CTC. This constraint also requires that the spacing between BF1 and CTC be as small as possible ($\leqq$0.32 cm) without making electrical contact. The entrance and exit apertures of CTC were made of copper and held between special knife-edged flanges by six 8-32, 304 stainless steel screws. The charge-transfer cell is supported with a tubulated ceramic-to-metal seal from CTCE. This tubulated ceramic-to-metal seal serves to isolate electrically the cell and screen elements; it also serves as the charge-transfer gas inlet port. CTCS was made from 50 × 50 tungsten wire mesh, tack welded to 304 stainless steel circular end rings. The end rings were 0.5 cm thick, had

a 1.16-cm outside diameter, and a 1.0-cm inside diameter. Three equally spaced holes were drilled through the end rings to a diameter of 0.28 cm and used for mounting CTCS with 0.32-cm-diameter sapphire balls placed in each hole to insulate electrically CTCS from CTC and to hold the CTCS symmetrically in place. The CTCS wire mesh was reinforced lengthwise with three thin pieces of 304 stainless steel strips, 0.13 cm wide, equally spaced, and tack welded to the screen wire and end rings.

The apparatus must be maintained in the 10^{-4}-Pa pressure range. This range was maintained by three separate pumping stations. The volume enclosing the mass spectrometer, lens 1 optic section, and T1 was maintained at working pressures of 2×10^{-4} Pa to 4×10^{-4} Pa by using a 5.08-cm (2-in.), 80-liter/sec oil-diffusion-pump and mechanical-pump arrangement. The volume enclosing the electrodes T2 through BF2 was maintained at working pressures of 5×10^{-5} Pa to 5×10^{-4} Pa by using a 400-liter/sec turbomolecular pump. Another 5.08-cm (2-in.), 80-liter/sec oil-diffusion and mechanical-pumping station was used to help evacuate the volume at the exit of the charge-transfer cell. Liquid nitrogen cryogenic traps were used with both diffusion pumps.

CHARGE-TRANSFER GAS PRESSURE MEASUREMENT

The gas pressure in CTC must be known accurately in the calculation of charge-transfer cross sections. Any errors associated with pressure measurements are transferred to cross-section data. Several direct pressure sensing devices, such as ionization gages, McLeod gages, and capacitance manometers, have been used. Each device requires connection to CTC through a somewhat restricted tubulation. Inherent errors are associated with this method because of the conductance of the connecting tubing that is usually not considered. As an example, a connecting tube of 0.64-cm diameter and 15 cm long has a conductance of approximately 0.21 liter/sec for N_2 at 298 K. An indicated pressure of 10^{-2} Pa at the pressure sensor would then correspond to a pressure of 0.14×10^{-2} Pa in CTC, where the CTC aperture conductance has been taken to be the calculated value of 1.47 liters/sec for free-molecular flow conditions. If the conductance of the connecting tubing were not taken into consideration in the pressure measurement, it would represent an error of 86 percent. Additional problems were encountered with ionization gages because of stray charged particles interfering with the current measurement. The problem of connecting tubing was eliminated by using a porous-leak conductance measurement technique described in reference 1. Figure 1 shows the connection of the porous metal leak to CTC and the capacitance manometer as a pressure sensor on the high-pressure side of the leak. With this arrangement the capacitance manometer is operated at a pressure of 1.33×10^{3} Pa to 1.33×10^{4} Pa where the accuracy is better than 0.03 percent. Calibrated data for the porous metal leak were obtained. The conductance was determined from these data to be 9.74×10^{-6} liter/sec for N_2 at ambient temperature. The conductance of the porous metal leak is much less than the conductance (0.2 liter/sec) of the connecting tubing; therefore, conductances associated with connecting tubing can be ignored.

The charge-transfer gas in CTC can now be monitored by using the porous-metal-leak gas inlet system of a known conductance. The entrance and exit

aperture of CTC are the sharp-edge type, machined with precision from oxygen-free high-conductivity (OFHC) copper. Since the apertures of CTC are the nearly ideal sharp-edge type, their conductance is readily calculable by using equations for a Maxwellian gas under free-molecular flow conditions (ref. 6). The CTC and the porous-metal-leak inlet system are connected by a vacuum-tight bellows and flange arrangement such that the pressure in the CTC is known at any time by considering molecular conservation of gas flow from which is obtained (ref. 7)

$$p_p C_p = C_{CTC} p_{CTC} \tag{3}$$

where p_p is the pressure on the high-pressure side of the porous metal leak and is monitored at all times; C_p and C_{CTC} are the conductances of the porous metal leak and charge-transfer cell apertures, respectively; p_{CTC} is the pressure inside CTC, and its value is needed for making charge-transfer cross-section calculations.

CURRENT MEASUREMENT

Charge-transfer cross sections are given by the equation

$$\sigma = -\frac{kT}{p_{CTC}} \frac{dI(x)}{I(x)\,dx} \tag{4}$$

Rearrangement and integration of equation (4) leads to the following Beer-Lambert (ref. 8) expression

$$I(x) = I(x=0)\, \exp\left(-\frac{p_{CTC}}{kT}\sigma x\right) \tag{5}$$

From equation (5)

$$\sigma = -\frac{kT}{p_{CTC} x} \ln \frac{I(x)}{I(x=0)} \tag{6}$$

where σ represents the total macroscopic scattering cross section for processes by which ions are lost. In equations (4), (5), and (6) the ideal gas law has been utilized to substitute for the neutral gas number density in the charge-transfer cell. In charge-transfer cross-section measurement experiments, the part of the transmitted beam current that does not undergo a charge-transfer process or scattering must be known. The transmitted current is given by

$$I(x) = I(x=0) - I_{CT} \tag{7}$$

In equation (7) I_{CT} represents that portion of the incident current related to the charge-transfer process; it is a current associated with the slow ions formed in the charge-transfer collisions. From equations (6) and (7)

$$\sigma = -\frac{kT}{p_{CTC}x} \ln\left[1 - \frac{I_{CT}}{I(x=0)}\right] \tag{8}$$

In order to apply equation (8), a detection and collection scheme had to be developed to separate the slow ions produced by charge transfer from the more energetic ions. The detection and collection scheme used is shown in figure 5. The quantity I_{CT} in equation (8) represents that portion of incident current related to the charge-transfer process; it is a current associated with the slow ions formed in charge-transfer collisions. Charge-transfer ions I_{CT} are collected on the charge-transfer cell screen (CTCS) by maintaining a negative potential $\Delta\phi$ between CTCS and CTC. A small fraction of the primary beam will also be collected on CTCS because the screen wire is not completely transparent to those few primary ions scattered through a large enough angle along the beam path. Under ideal focusing conditions, all primary ions that do not undergo charge transfer would pass through CTC and be collected at beam flag 2 (BF2). Because of imperfection in focusing and apparatus alinement, this condition was never obtained. In figure 6 the experimental values of the current ratio $I_{CTCS}/I(x=0)$ show a dependence on the value of the voltage $\Delta\phi$. Since the current ratios are used in the calculation of charge-transfer cross sections, observed cross sections will also have a $\Delta\phi$ dependence. By plotting the current ratio $I_{CTCS}/I(x=0)$ as a function of $\Delta\phi$ from 0 to 12 volts, a curve that increases in a nonlinear fashion from 0 to 2 volts is obtained and is essentially flat from 2 to 12 volts (fig. 6). The flat portion of the curve gives the saturation current ratio, which is referred to as $I_{CTCS}/I(x=0)\big|_S$.

The corresponding measured value of the current ratio at $\Delta\phi = 0$ is referred to as $I_{CTCS}/I(x=0)\big|_0$. When there are no electric fields within the charge-transfer cell, $\Delta\phi$ is equal to zero. The slow ion current collected on the CTC and the CTCS when $\Delta\phi = 0$ will be determined by the relative areas of these elements. For the purposes of discussion, the ion currents to the CTC and the CTCS can be divided into two components: The fast ions from the primary beam which impinge on both the CTC and the CTCS; and the slow ions which are the products of charge transfer. For the slow ions the areas of the CTCS and CTC are in the ratio of about 8:92 based on the CTCS transparency and the surface area of CTC. Therefore, about 8 percent of the slow ions will be collected at CTCS, when $\Delta\phi = 0$. The magnitude of the slow ions current is always much less than that of the fast ions current. This inequality is enhanced by the geometric character of the collection process when $\Delta\phi = 0$; therefore the current ratio $I_{CTCS}/I(x=0)\big|_0$ can be considered to represent essentially only fast ions. When $\Delta\phi$ is large, essentially all slow ions are collected as shown by the saturation in the growth of $I_{CTCS}/I(x=0)$ as a function of $\Delta\phi$ in figure 6. Therefore, the collection of fast ions is not affected by the relatively small magnitudes of $\Delta\phi$ used in this study. Thus, in the limit of large $\Delta\phi$ (12 volts), the current ratio $I_{CTCS}/I(x=0)\big|_S$ is the sum of all the slow ions collected plus a fast ion contribution given as

$$\left.\frac{I_{CTCS}}{I(x=0)}\right|_S = \frac{I_{CT}}{I(x=0)} + \frac{I_F}{I(x=0)} \tag{9}$$

From the preceding discussion, note that

$$\frac{I_F}{I(x=0)} = \left.\frac{I_{CTCS}}{I(x=0)}\right|_0 \tag{10}$$

Therefore, from equation (10)

$$\frac{I_{CT}}{I(x=0)} = \left.\frac{I_{CTCS}}{I(x=0)}\right|_S - \left.\frac{I_{CTCS}}{I(x=0)}\right|_0 \tag{11}$$

In the calculations of charge-transfer cross sections, it was necessary to refer to the current ratio measurements in the limit where $\Delta\phi = 0$. This calculation was done by employing an extrapolation technique illustrated in figure 6. Figure 5 shows that

$$\phi_{IE} = \phi_{IAV} - \phi_{CTC} + \Delta\phi \tag{12}$$

For all data given in reference 1 and related to charge transfer, the quantity $\phi_{IAV} - \phi_{CTC}$ was recorded as the nominal ion energy potential. From the preceding discussion, the expression for cross sections given by equation (8) becomes

$$\sigma = -\frac{kT}{p_{CTC}x} \ln\left[1 + \left.\frac{I_{CTCS}}{I(x=0)}\right|_0 - \left.\frac{I_{CTCS}}{I(x=0)}\right|_S\right] \tag{13}$$

PROBABLE ERRORS IN MEASUREMENT TECHNIQUES

As indicated previously, the charge-transfer cross section is given by

$$\sigma = -\frac{kT}{p_{CTC}x} \ln\left[1 - \frac{I_{CT}}{I(x=0)}\right] \tag{14}$$

In order to obtain the effects of uncertainty in all parameters, experimental values had to be substituted in equation (14). By using the procedure detailed in reference 1, the overall uncertainty in the cross-section values is given by

$$\frac{\Delta\sigma}{\sigma} = \left(\left(\frac{3\ \Delta T}{2T} \right)^2 + \left(\frac{2\ \Delta r_1}{r_1} \right)^2 + \left(\frac{2\ \Delta r_2}{r_2} \right)^2 + \left(\frac{\Delta t}{t} \right)^2 + \left(\frac{\Delta V}{V} \right)^2 \right.$$

$$+ \left(\frac{\Delta x}{x} \right)^2 + \left(\frac{\Delta p_p}{p_p} \right)^2 + \left(\frac{\Delta p_o}{p_o \ln p_o/p_f} \right)^2 + \left(\frac{\Delta p_f}{p_f \ln p_o/p_f} \right)^2$$

$$+ \left\{ \frac{\Delta I_{CT}}{I(x=0)\left[1 - I_{CT}/I(x=0)\right] \ln \left[1 - I_{CT}/I(x=0)\right]} \right\}^2$$

$$\left. + \left\{ \frac{I_{CT}\ \Delta I(x=0)}{I^2(x=0)\left[1 - I_{CT}/I(x=0)\right] \ln \left[1 - I_{CT}/I(x=0)\right]} \right\}^2 \right)^{1/2} \qquad (15)$$

For the sake of specificity the overall errors in σ were calculated by using the parameter values listed in table I. Substituting these values in equation (15), the fractional error in σ is found to be 5.7 percent. An additional error is not exhibited in equation (15). This error enters in the current collection process as described in reference 1. When $\Delta\phi = 0$, the current measured at CTCS is given by the relation $I_{CTCS} = 0.11I_{slow} + 0.43I(x=0)$. When $\Delta\phi = 12$ volts, the current measured at CTCS is given by a different relation $I_{CTCS} = I_{slow} + 0.43I(x=0)$. The current ratio $ICT/I(x=0)$ is defined by

$$\frac{I_{CT}}{I(x=0)} = \left. \frac{I_{CTCS}}{I(x=0)} \right|_S - \left. \frac{I_{CTCS}}{I(x=0)} \right|_0 \qquad (16)$$

It follows that

$$I_{CT} = \left[I_{slow} + 0.43I(x=0) \right] - \left[0.11I_{slow} + 0.43I(x=0) \right] = 0.89I_{slow}$$

The actual measured value of the slow ion current is 89 percent of the true value of slow ion current. When this error is considered in the cross-section equation, $(\sigma_T - \sigma_M)/\sigma_T = 11$ percent, where σ_T is considered to be the true value, and σ_M, the measured value. When the error due to current collection is added to the systematic errors given by equation (16), the total fractional error is found to be in the range of $0.057 < \Delta\sigma/\sigma < 0.167$. The errors quoted here are attributed to parameter measurements only. Other errors associated with theoretical equations have not been considered in these computations.

CONCLUDING REMARKS

An experimental apparatus that can be used in ion-molecule collisional-type studies has been briefly described. Charge-transfer cross sections are obtained in an ion-molecule collision by measuring the appropriate currents associated with the charge-transfer process and the pressure in the charge-transfer cell. From this study it is apparent that, in any charge-transfer apparatus, a technique of separation and collection of slow ion current and fast primary ions must be devised. In this work a technique of separation and collection of both slow and fast ions has been developed.

Accurate pressure measuring techniques are also needed to know adequately the static gas pressure within the charge-transfer cell. Measurement errors associated with the pressure are directly transferrable to the charge-transfer cross sections. In this work a porous-metal-leak technique was used to determine the pressure in the charge-transfer cell. This technique is superior to other methods of pressure measurement, such as ionization gages, McLeod gages, and pressure sensors connected directly to the charge-transfer cell. The porous-metal-leak technique of pressure measurement has not been used in other charge-transfer apparatus heretofore. An error analysis for the experimental measurement parameters indicates that the fractional measurement error for this technique is in the range of 6 to 17 percent.

Charge-transfer techniques can be extended and used in aerospace research problems in the following applications:

1. Ion-molecule reaction-rate data as a function of ion energy.

2. Ions and gas-surface interactions as a function of ions and neutral beam energy.

3. Measuring gas-surface accommodation coefficients.

4. Use a high-velocity neutral gas beam to simulate reentry-vehicle atmospheric conditions.

Langley Research Center
National Aeronautics and Space Administration
Hampton, VA 23665
July 18, 1978

REFERENCES

1. Smith, Alphonsa: Studies of Charge Transfer in the $N_2^+ - N_2$ System. Ph. D. Diss., Virginia Polytechnic Institute and State University, May 1977.

2. Mason, Edward A.; Vanderslice, Joseph T.; and Yos, Jerrold M.: Transport Properties of High-Temperature Multicomponent Gas Mixtures. Phys. Fluids, vol. 2, no. 6, 1959, pp. 688-694.

3. Nichols, Billy J.; and Witteborn, Fred C.: Measurements of Resonant Charge Exchange Cross Sections in Nitrogen and Argon Between 0.5 and 17 EV. NASA TN D-3265, 1966.

4. Schissel, P. O.; and Trulson, O. C.: Mass-Spectrometric Study of the Oxidation of Tungsten. J. Chem. Phys., vol. 43, no. 2, 1965, pp. 737-743.

5. McDaniel, E. W.; Čermák, V.; Dalgarno, A.; Ferguson, E. E.; and Friedman, L.: Ion-Molecule Reactions. Wiley-Interscience, c.1970, pp. 4-28.

6. Dushman, Saul (J. M. Lafferty, ed.): Scientific Foundations of Vacuum Technique. Second ed. John Wiley & Sons, Inc., c.1962, p. 90.

7. Guthrie, A.; and Wakerling, R. K., eds.: Vacuum Equipment and Techniques. McGraw-Hill Book Co., Inc., 1949, pp. 12-27.

8. Bederson, Benjamin; and Fite, Wade L., eds.: Atomic and Electron Physics - Atomic Interactions. Volume 7 (Part A) of Methods of Experimental Physics, Academic Press, 1968, p. 143.

TABLE I.- MEASUREMENT UNCERTAINTY DATA

Parameter, X	Differential factor, $\frac{1}{\sigma}\frac{\partial\sigma}{\partial X}$	Measurement uncertainty, ΔX
$T = 295$ K	$3/2T$	2K
$r_1 = 0.119$ cm	$2/r_1$	0.0015 cm
$r_2 = 0.159$ cm	$2/r_2$	0.0015 cm
$t = 1.26 \times 10^4$ sec	$1/t$	5 sec
$V = 241$ cm^3	$-1/V$	2 cm^3
$x = 5.08$ cm	$-1/x$	0.18 cm
$p_p = 4 \times 10^3$ Pa	$-1/p_p$	2.6 Pa
$p_o = 1.33 \times 10^5$ Pa	$-\frac{1}{p_o \ln p_o/p_f}$	8.0 Pa
$p_f = 8 \times 10^3$ Pa	$\frac{1}{p_t \ln p_o/p_f}$	4.8 Pa
$I_{CT} = 1.5 \times 10^{-10}$ A	$\frac{-1}{I(x=0)\left[1 - I_{CT}/I(x=0)\right] \ln \left[1 - I_{CT}/I(x=0)\right]}$	3×10^{-12} A
$I(x=0) = 17.3 \times 10^{-10}$ A	$\frac{I_{CT}}{I(x=0)^2\left[1 - I_{CT}/I(x=0)\right] \ln \left[1 - I_{CT}/I(x=0)\right]}$	3.46×10^{11} A

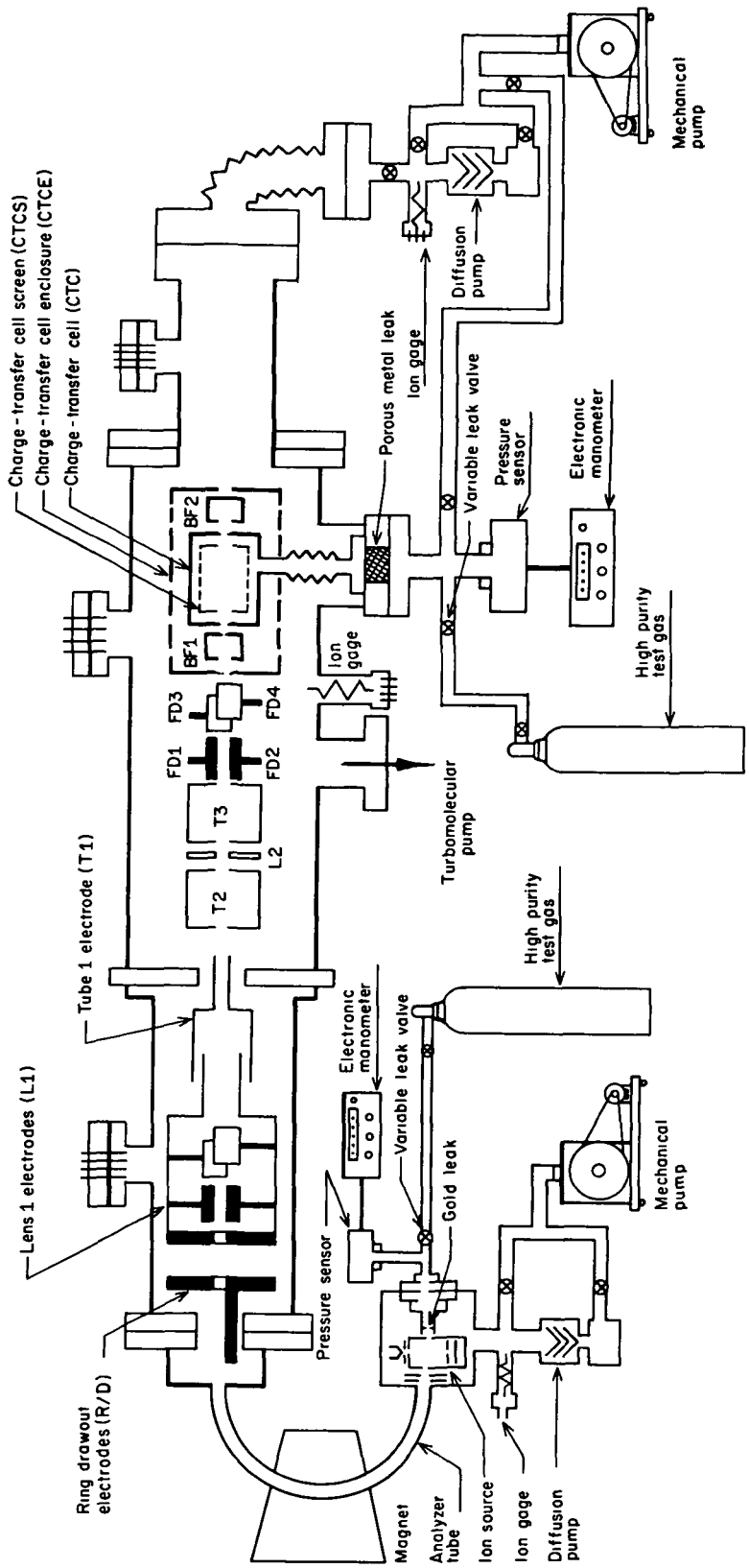

Figure 1.- Schematic diagram of total system.

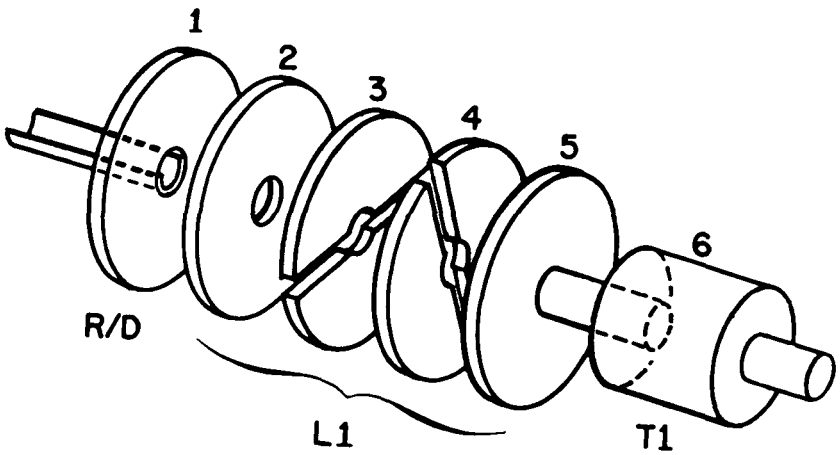

Figure 2.- Ion-optics section 1.

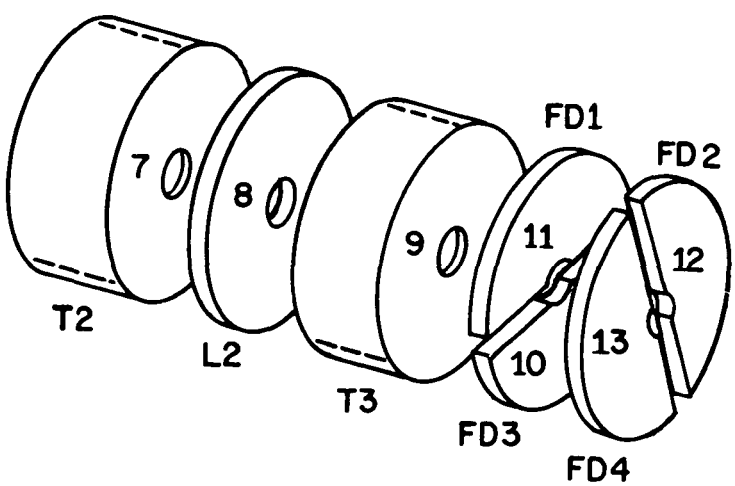

Figure 3.- Ion-optics section 2.

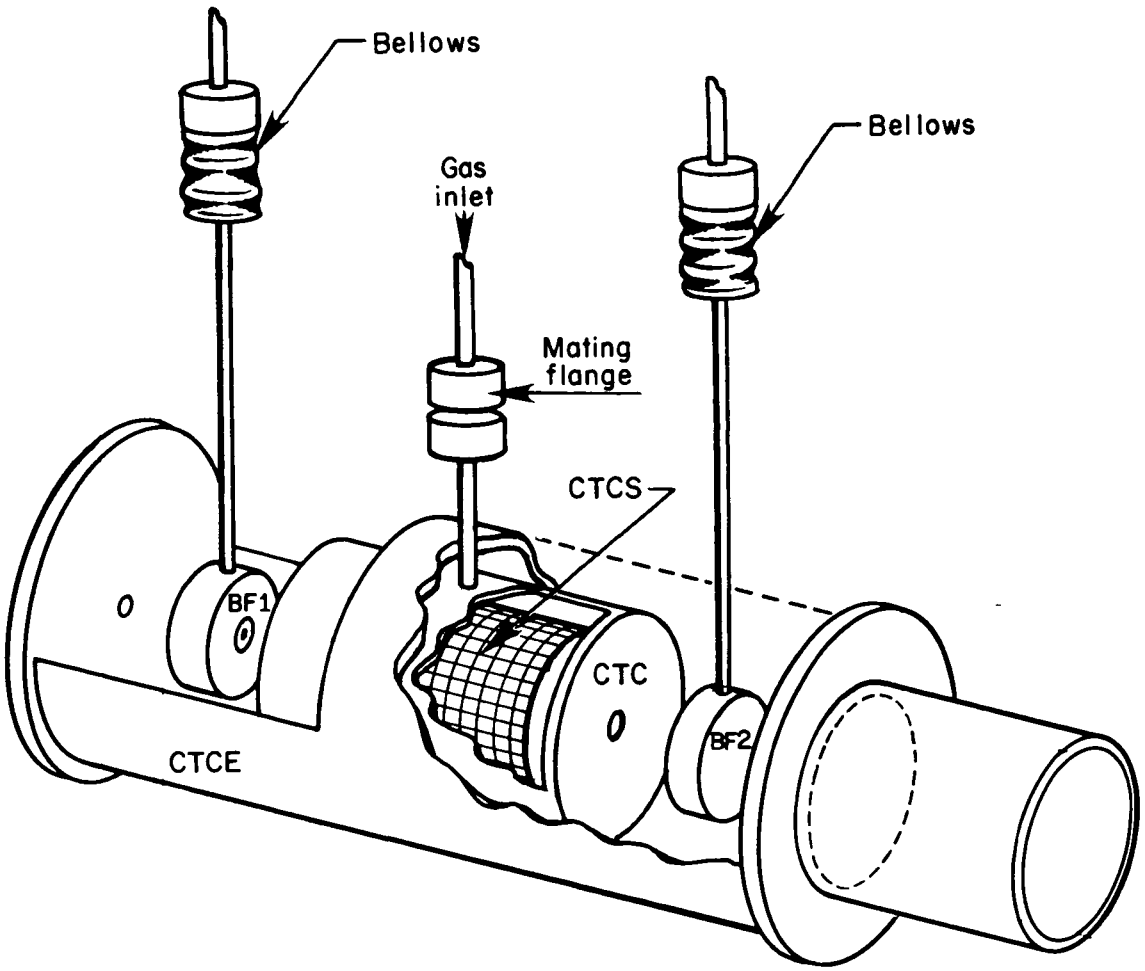

Figure 4.- Charge-transfer cell section.

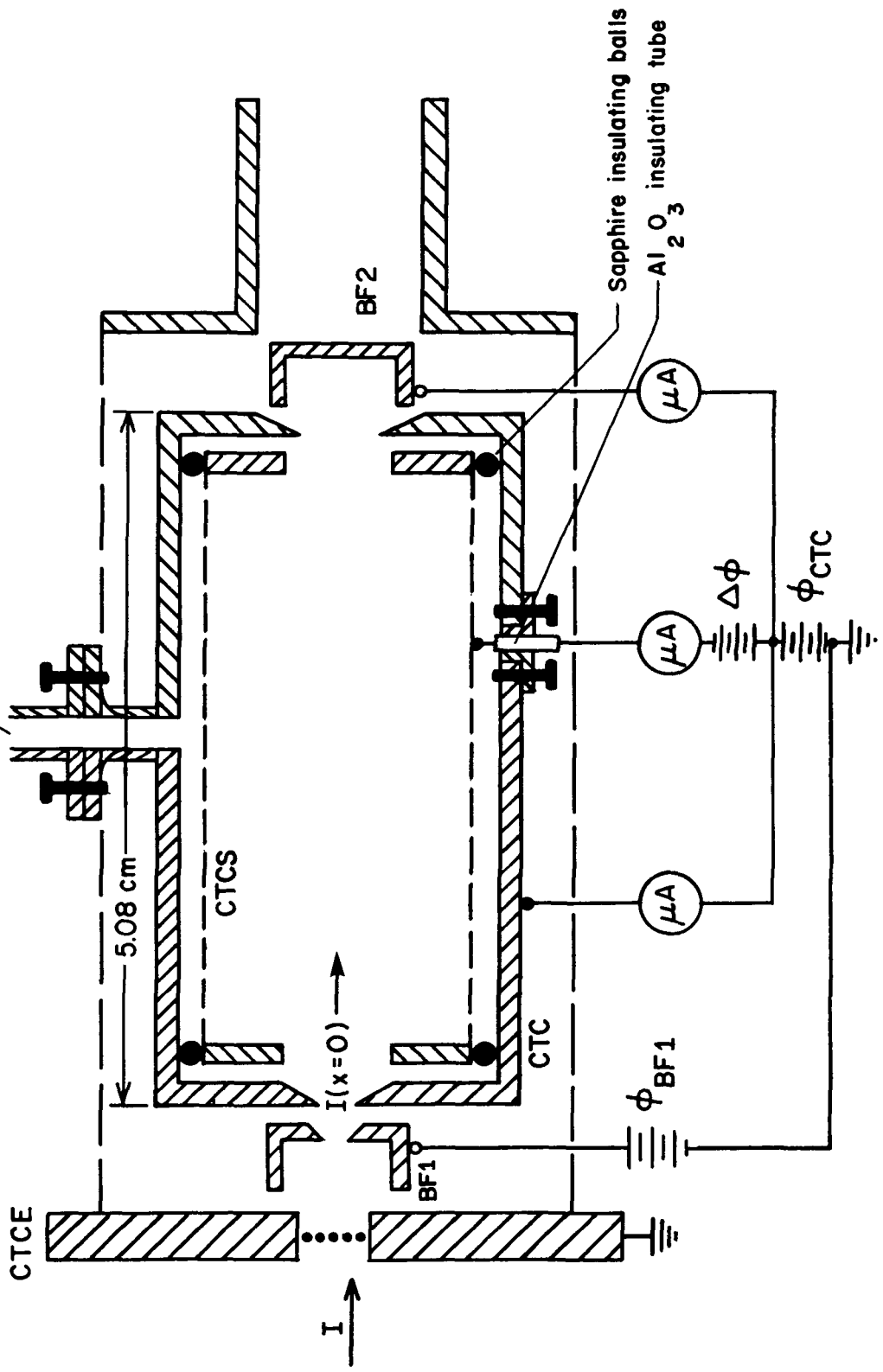

Figure 5.- Ion detection and collection system.

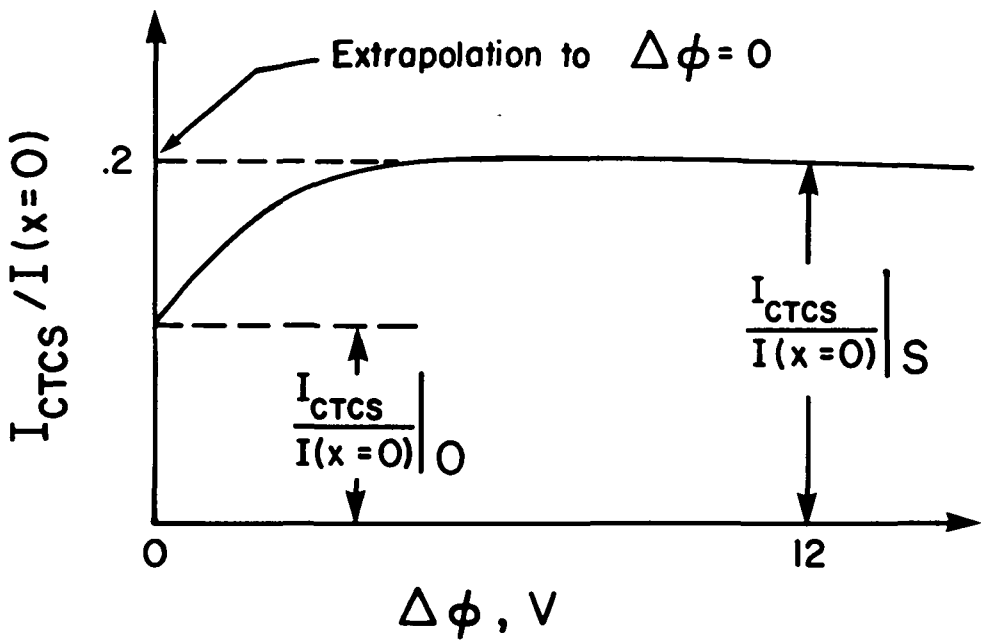

Figure 6.- Typical experimental behavior of current ratio $I_{CTCS}/I(x=0)$ plotted against $\Delta\phi$.

1 Report No.	2 Government Accession No	3. Recipient's Catalog No.
NASA TM-78734		

4 Title and Subtitle	5 Report Date
MEASUREMENT TECHNIQUES AND APPLICATIONS OF CHARGE TRANSFER TO AEROSPACE RESEARCH	September 1978
	6 Performing Organization Code
7 Author(s)	8 Performing Organization Report No
Alphonsa Smith	L-12278
9 Performing Organization Name and Address	10 Work Unit No
NASA Langley Research Center	505-07-23-07
Hampton, VA 23665	11 Contract or Grant No
	13 Type of Report and Period Covered
12 Sponsoring Agency Name and Address	Technical Memorandum
National Aeronautics and Space Administration	
Washington, DC 20546	14 Sponsoring Agency Code

15 Supplementary Notes

16 Abstract

A technique of developing high-velocity low-intensity neutral gas beams for use in aerospace research problems is described. This technique involves ionization of gaseous species with a mass spectrometer and focusing the resulting primary ion beam into a collision chamber containing a static gas at a known pressure and temperature. Equations are given to show how charge-transfer cross sections are obtained from a total-current measurement technique. Important parameters are defined for the charge-transfer process.

17 Key Words (Suggested by Author(s))	18 Distribution Statement
Charge transfer Molecular beams Current measurement	Unclassified - Unlimited Subject Category 35

19 Security Classif. (of this report)	20 Security Classif (of this page)	21. No. of Pages	22 Price*
Unclassified	Unclassified	18	$4.00

* For sale by the National Technical Information Service, Springfield, Virginia 22161

NASA-Langley, 1978

National Aeronautics and
Space Administration

Washington, D.C.
20546

Official Business
Penalty for Private Use, $300

SPECIAL FOURTH CLASS MAIL
BOOK

Postage and Fees Paid
National Aeronautics and
Space Administration
NASA-451

U.S.MAIL

6 1 1U,D, 082178 S00673HU
NORTHROP UNIV
ATTN: ALUMNI LIBRARY
1155 WEST ARBOR VITAE ST
INGLEWOOD CA 90306

NASA

POSTMASTER: If Undeliverable (Section 158
Postal Manual) Do Not Return